

22-Year magnetic solar cycle [Hale cycle] responsible for significant underestimation of the Sun's role in global warming but ignored in climate science

Martijn van Mensvoort

Key Points:

- 22-year Hale cycle solar minima show for the period 1890-1985 a high SST solar sensitivity (1,143 °C per W/m²)
- 22-year Hale cycle temperature profile amplitude (0,215 °C) is higher than for the 11-year Schwabe cycle (0,122 °C)
- Solar influence on climate is underestimated without a 22-year Hale cycle temperature correction ($\sim 0,1$ W/m²)

Corresponding author: Martijn van Mensvoort, martijn.van.mensvoort@gmail.com

Abstract

Reconstructions for global temperature development show an upward oscillation for the period of the 1880s through 1980s. This oscillation is being associated with natural variability and the temperature rise between the 1910s and 1940s with increased solar activity. The temperature impact of the 11-year solar cycle [Schwabe cycle] and the physical mechanism involved are insufficiently understood. Here, for the 22-year magnetic solar cycle [Hale cycle] a seawater surface temperature [SST] impact is described of $0,215^{\circ}\text{C}$ ($0,238 \pm 0,05^{\circ}\text{C}$ per W/m^2); the derived impact for the 11-year cycle is $0,122^{\circ}\text{C}$ ($0,135 \pm 0,03^{\circ}\text{C}$ per W/m^2). Also, a parallel development is described for seawater surface temperature [HadSST3 dataset] and the minima of total solar irradiance [LISIRD dataset] after a correction based on the 22-year solar cycle polarity change. With the correction, the combination of the positive and negative minima shows for the period 1890-1985 a high SST solar sensitivity: $1,143 \pm 0,23^{\circ}\text{C}$ per W/m^2 (with 90,5% declared variance). This implies that the Sun has caused a warming of $1,07^{\circ}\text{C}$ between Maunder minimum (late 17th century) and the most recent solar minimum year 2017 - which is well over half of the intermediate temperature rise of approximately $1,5^{\circ}\text{C}$. The results demonstrate that the 22-year cycle forms a crucial factor required for better understanding the Sun-temperature relation. Ignoring the 22-year cycle leads to significant underestimation of the Sun's influence in climate change combined with an overestimation of the impact of anthropogenic factors and greenhouse gases such as CO_2 .

Plain Language Summary

Global temperature development shows an upward oscillation for the 1880s through 1980s. This oscillation is associated with natural variability: increased solar activity largely explains the temperature rise between the 1910s and 1940s. However, the temperature impact of the 11-year solar cycle is insufficiently understood. Here, for the 22-year magnetic solar cycle a seawater surface temperature impact is described of $0,215^{\circ}\text{C}$, while the derived impact for the 11-year cycle is only $0,122^{\circ}\text{C}$. Also, a parallel development is described for seawater surface temperature and the minima of total solar irradiance, after a correction based on the 22-year solar cycle polarity change. With this correction, the combination of the positive and negative minima shows for the period 1890-1985 a high solar sensitivity for seawater surface temperature: $1,143^{\circ}\text{C}$ per W/m^2 . This also implies that the Sun caused a warming of $1,07^{\circ}\text{C}$ between Maunder minimum and solar minimum year 2017, well over half of the intermediate temperature rise of approximately $1,5^{\circ}\text{C}$. The 22-year cycle forms a crucial factor for better understanding the Sun-temperature relation. Ignoring the 22-year cycle leads to underestimation of the Sun's influence in climate change (+ overestimation of anthropogenic factors and greenhouse gases such as CO_2).

1 Introduction

In a 2006 Dutch scientific report by the Royal Netherlands Meteorological Institute (KNMI) in collaboration with the NIOZ, is reported that prior to 1950 the influence of humans on temperature had been negligible (de Jager et al., 2006). This makes the period prior to 1950 ideally suited for studying the influence of the Sun on temperature. In the current research, the influence of the Sun on seawater surface temperature is being studied for the period 1890-1985. This time frame includes 3 periods in which the temperature trend has changed direction plus it includes a total of 10 solar minimum years. According to experts, prior to 1880 insufficient data is available for a reliable estimate of the global seawater surface temperature; only after the year 1950 the uncertainty margin decreases to a low level for most regions of the world (Smith & Reynolds, 2003). Among experts there is consensus that the heat content of the ocean system is probably the best indicator of global warming (Cheng et al., 2019); logically, the warm-

ing of the seawater surface temperature is therefore probably a more relevant indicator than the warming of the atmosphere. In this study the HadSST3 dataset is used for seawater surface temperature.

There is controversy about the solar influence on climate on a wide range of aspects. Estimates for the temperature effect of the 11-year solar cycle [Schwabe cycle] vary from less than 0,05 °C (barely recordable) (de Jager et al., 2006) to more than 0,25 °C (Camp & Tung, 2007). However, a much larger temperature effect is expected for the same amount of energy when it involves a much longer timespan. For a 200-year cycle, the temperature effect is 2 to 4 times larger than for the 11-year cycle, particularly due to accumulation of energy within the ocean system (de Jager et al., 2006); for even longer periods the impact can be 5 to 10 times larger (Shaviv, 2005, 2012). This implicates that solar sensitivity (= the temperature response to solar activity) represents a complicated phenomenon because times scale and solar cycle phase is required to be taken into account. Additionally, the impact of a solar amplification factor (of unknown size) for the TSI signal measured at the top of the atmosphere should also be taken into consideration.

The controversy also concerns the share of the Sun in the 0,8 °C warming in the 20th century: available estimates range from 7% (0,056 °C) to 44-64% (0,35-0,51 °C) (Scafetta, 2013). The compilation method of the historical dataset for total solar irradiance [TSI] is an important part of the controversy as well (Solanki et al., 2013). Since the 1990s, even the scientific legitimacy has been debated in relation to the compilation method used by different research groups involved; among experts this issue is known as the ACRIM-PMOD controversy (Scafetta et al., 2019). Large opinion differences have arisen with regard to the TSI construction method. The widely adopted method of Lean (Lean et al., 1995) is based on just 2 magnetic components and produces a curve which shows the highest TSI values in the late 1950s. While, for example, the method of Hoyt & Schatten (Hoyt & Schatten, 1993) is based on 5 magnetic components and produces a curve which shows the highest TSI values near the beginning of the 21st century. This means that estimates for the influence of the Sun on the climate differ both numerically and fundamentally to a great extent; numerically, the controversy involves impact differences of nearly a factor of 10.

In climate science the influence of the Sun is studied, among other things, by means of the 11-year solar cycle. However, fundamentally, it has been established since the beginning of the 20th century that the 22-year magnetic solar cycle [Hale cycle] forms the origin of the 11-year sunspotcycle (Hale, 1908). This is important because two consecutive 11-year cycles exhibit structural differences; an illustrative example for this involves the Gnevyshev-Ohl rule (Zolotova & Ponyavin, 2015), which relates to the number of sunspots between 2 consecutive maximums. It is therefore remarkable that the 22-year cycle is hardly taken into consideration in climate science. IPCC reports do not mention the existence of the 22-year Hale cycle (Hiyehara et al., 2008). Descriptions elsewhere in the scientific literature indicate that manifestations of the 22-year cycle are being presumed to be not sensitive to the polarity change; however, the foundation for such assumptions is unclear. Because, for example, in 2008 it has been determined that since Maunder minimum the coldest phase of the 22-year cycle takes place (under the influence of cosmic rays) during the minima that occur when the polarity is positive; the magnetic solar poles are then located in their original position (IPCC, 2013; Hiyehara et al., 2008).

This study therefore distinguishes two categories of solar minima (Mursula & Hiltula, 2003): (1) positive minima [P], which arise during the phase when the magnetic polarity of the northern solar hemisphere is positive with both poles in the original position; and (2) the negative minima [N], which arise during the phase when the magnetic polarity of the northern solar hemisphere is negative with switched positions for both poles. This is crucial because solar radiative forcing trend analysis is usually based on solar minimum years because the phase of the solar cycle must be taken into account (in order

to avoid effects that origin from phases differences in the solar cycle). Solar sensitivity is typically higher for long term perspectives; therefore especially for periods much longer than the 11/22-year solar cycle the phase of the solar cycle needs to be considered in order to separate trend effects due to the 11/22-year solar cycle from trend effect in longer term perspectives. This is explained by the fact that minima are both "more stable" and "more relevant" than maxima (IPCC, 2013). IPCC AR5 presents a definition for the TSI which refers only to the minima. In terms of the physical processes involved this is explained by the fact that the number of sunspots and solar flares is relatively small during the minima. Both represent the two magnetic components in the Lean method, which also represent the basis of the LISIRD TSI dataset used in this study. The maxima are accompanied by relatively large fluctuations, which exhibit higher uncertainty than the minima. This is because the result at the maxima depends more strongly on the magnetic components used in the reconstruction (Lean et al., 1995; Hoyt & Schatten, 1993). This explains the fundamental relevance of the choice made in this study to use the perspective of the solar minimum years as the most important point of reference for studying the climate impact of the 22-year magnetic solar cycle. Additionally, the sunspot convention is used in order to separate also two categories of solar maxima: (1) 'even maxima' [E] from (2) 'odd maxima' [O] (Ross & Chaplin, 2019). Figure 1 describes the Hale cycle based on Wilcox Solar Observatory data; the LISIRD TSI dataset is added for reference at the bottom.

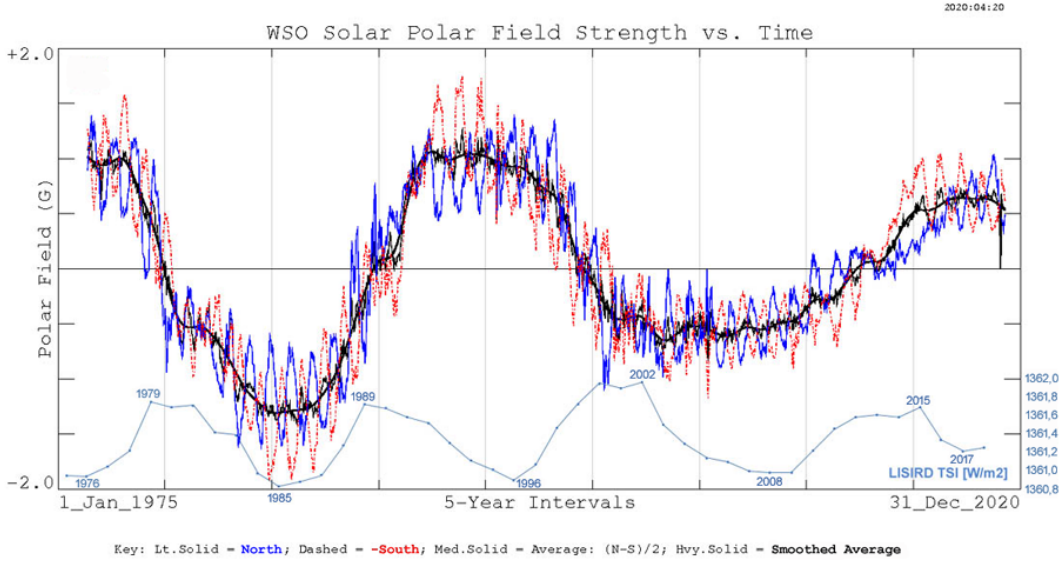


Figure 1. The amplitude of the poloidal solar magnetic field is largest during the years around the TSI minima; Wilcox Solar Observatory data shows that the field changes polarity during the TSI maxima (source: (*WSO: Solar Polar Field Strength [.gif]* <http://wso.stanford.edu/gifs/Polar.gif>)). The Lt.Solid (blue) and Dashed (red) graphs show activity of the magnetic north pole and inverted south pole, respectively; the Med.Solid (black) graph represents the average magnetic activity and the Hvy.Solid (bold black) graph represents the smoothed average. The LISIRD TSI is added at the bottom.

2 Materials and Methods

The materials used in this study involve datasets for global sea surface temperature and total solar irradiance. For global sea surface temperature is used the Hadley

Centre Sea Surface Temperature dataset [*HadSST3* : <https://www.metoffice.gov.uk/hadobs/hadsst3/data/download.html> (MetOffice, 2020)] presented by the Hadley Centre Met Office, who's sea surface temperature datasets serve in IPCC AR5 (IPCC, 2013). For total solar irradiance is used the Lasp Interactive Solar IRadiance Datacenter dataset: Historical Total Solar Irradiance Reconstruction, Time Series [*LISIRD*: http://lasp.colorado.edu/lisird/data/historical_tsi/ (Kopp, 2019)], which is an unofficial dataset presented by LASP principal investigator Dr. Greg Kopp. On Greg Kopp's TSI Page the LISIRD is being described to represent the best values available. The LISIRD uses for the pre-satellite period 1611-1978 the SATIRE-T TSI dataset with some refinements included (Kopp et al., 2016); for the satellite period 1979-2018 it used the Community-Consensus TSI Composite (Dudok de Wit et al., 2017). Though Kopp's LISIRD data set has no official status, his work as a lead researcher in solar irradiance assessment with satellites is featured with multiple references in IPCC AR5.

Because sea surface temperature is being claimed to be unreliable before 1880 due to insufficient data (Smith & Reynolds, 2003) and the ACRIM-PMOD controversy indicates that there are unsolved problems with TSI data starting from the mid-nineties minimum (Scafetta et al., 2019), the period 1880-1985 is used here as the main research period for studying the solar-climate connection. This choice is also justifiable because prior to 1950 the influence of humans on temperature had been negligible (de Jager et al., 2006); however, the HadSST3 dataset indicates that the rise of sea surface temperature started in the 2nd half of the 1970s.

The data analysis starts with a correlation assessment (based on Pearson correlation coefficient calculated with Excel) for the full data set (1880-2018) and the chosen research period (1880-1985), combined with an assessment focused on the solar minimum years and solar maximum years separately.

Then a temperature profile for the Hale cycle is constructed from the chosen research period (with 5 successive Hale cycles included). Average values for the two separate Hale cycle minima and the two separate Hale cycle maxima serve as reference points in order to construct the profile. A linear upward trend is first removed with an improvisation method (which is necessary due to the irregular length of the solar cycle) using the linear average upward directed trend during the period 1882-1988 in order to make sure that the beginning and ending of the Hale temperature profile show the same value. The slope of the applied trend removal has been checked to be a realistic value that is representative for the temperature rise in the period 1880-1985. The profile is then constructed based on consistent patterns between snippets of the profile found at the surrounding years near the minima and maxima.

Because the minima are known to represent the most stable and most relevant phase of the solar cycle, only the Hale cycle minima are then used to serve for studying the solar-climate connection in depth with the introduction of a correction based on the 22-year cycle solar polarity change. The use of a correction based on the 22-year Hale cycle involves an innovative element that has not been introduced before in reports focused on studying the solar-climate connection. This is initially done for just the minimum years involved, which requires a separation between positive and negative solar minimum years; analyses are made here based on the use of a correlation test combined with an explained variance test (based on R2 method via linear regression analysis + significance levels both calculated with PSPP software). The correction serves to neutralize a structural temperature difference between the positive and negative solar minimum years. An additional analysis is also presented for Hale cycle minima based on multiple years 3 up to 9 years; an analysis based on 11-year minima is presented as well but it is not taken into consideration for analysis due to overlap between various periods (because for 11-year minima periods some years become included in multiple minima periods - which is obviously not acceptable).

Finally, the SST solar sensitivity is calculated for 3 different perspectives (at the top at the atmosphere, for earth surface after adjusting for the shape of the earth & albedo without an amplification factor, and for earth surface after adjusting for the shape of the earth & albedo with an amplification factor). These 3 perspectives are described for the minima period 1890-1985, for the 22-year cycle and for the 11-year cycle.

The data analysis is available as a spreadsheet. The section 'Electronic Supplementary Material' presents online resources available in 2 formats: in (1) Excel format (data + results including calculations) and in (2) CSV format (data + results excluding calculations). The files are available at a repository download location. The spreadsheet describes for the period 1880-2019 the LISIRD TSI dataset + the HadSST3 dataset + all correlations (based on Pearson correlation coefficient) + all explained variances (based on R2 method via linear regression) featured in figures 2 through 5. For the purpose of reproducibility a detailed summary is presented for each of these figures; the data shown in each figure is processed in the data files as follows:

- Figure 2: LISIRD TSI (column C), HadSST3 (column D); columns I to AW show data + correlations with regard to the periods 1880-2018 and 1880-1985 for: maxima, odd maxima [O], even maxima [E], minima, positive minima [P], and negative minima [N].
- Figure 3: Temperature profile Hale cycle (column CW), temperature profile Schwabe cycle (column CZ); columns BB to CS present the underlying calculation method for the Hale cycle temperature profile. The Hale cycle temperature profile is composed of 4 series of data around the TSI minima and maxima years, whereby the profile of the positive minima years is split into 2 parts (column BX and column CN therefore contain the same data). The trend has been removed from each of the 4 reference profiles based on a slope corresponding to a temperature increase of 0,0028 °C per year (= 0,28 °C per 100 years); a higher or lower value would mean that the second positive minimum (for year 22) in figure 3 would not end exactly at zero. Only the values labeled with a * have been processed in the Hale cycle temperature profile. The indicative bandwidths (column DF for the negative minimum, column DH for the temperature peak year) represent the outliers derived from 4 successive full Hale cycles based on the period 1890-1976. The Schwabe cycle temperature profile has been derived from the Hale cycle temperature profile.
- Figure 4: [TOP] LISIRD (column EI), HadSST3 (column EJ); [BOTTOM] LISIRD with corrected negative minima (column EQ), HadSST3 (column ER). The correction value is the lowest value, for which the average correlation value of the positive and negative data combined is found.
- Figure 5: 1-year mean corrected LISIRD (column FR) & HadSST3 (column FS); 3-year mean corrected LISIRD (column GQ) & HadSST3 (column GR); 5-year mean corrected LISIRD (column HP) & HadSST3 (column HQ); 7-year mean corrected LISIRD (IO column) & HadSST3 (IP column); 9-year mean corrected LISIRD (column JN) & HadSST3 (column JO); 11-year mean corrected LISIRD (column KM) & HadSST3 (column KN). The correction value represents the lowest value for each minimum period whereby for the minima combination the average correlation value of the positive and negative data is found.

3 Results

With the Hale cycle taken in consideration, correlations between TSI and seawater surface temperature are described first. The period around the minimum years 1890

to 1985 is then used in order to calculate the temperature profile for the 22-year Hale cycle (+ the temperature profile for the 11-year Schwabe cycle). Also, based on the minimum years a description for the solar sensitivity in the long-term perspective is presented. A distinction is made between: (1) 'primary minima' which are formed during the phase with the magnetic poles in the original position and (2) 'secondary minima' which are formed during the phase when the poles have switched positions.

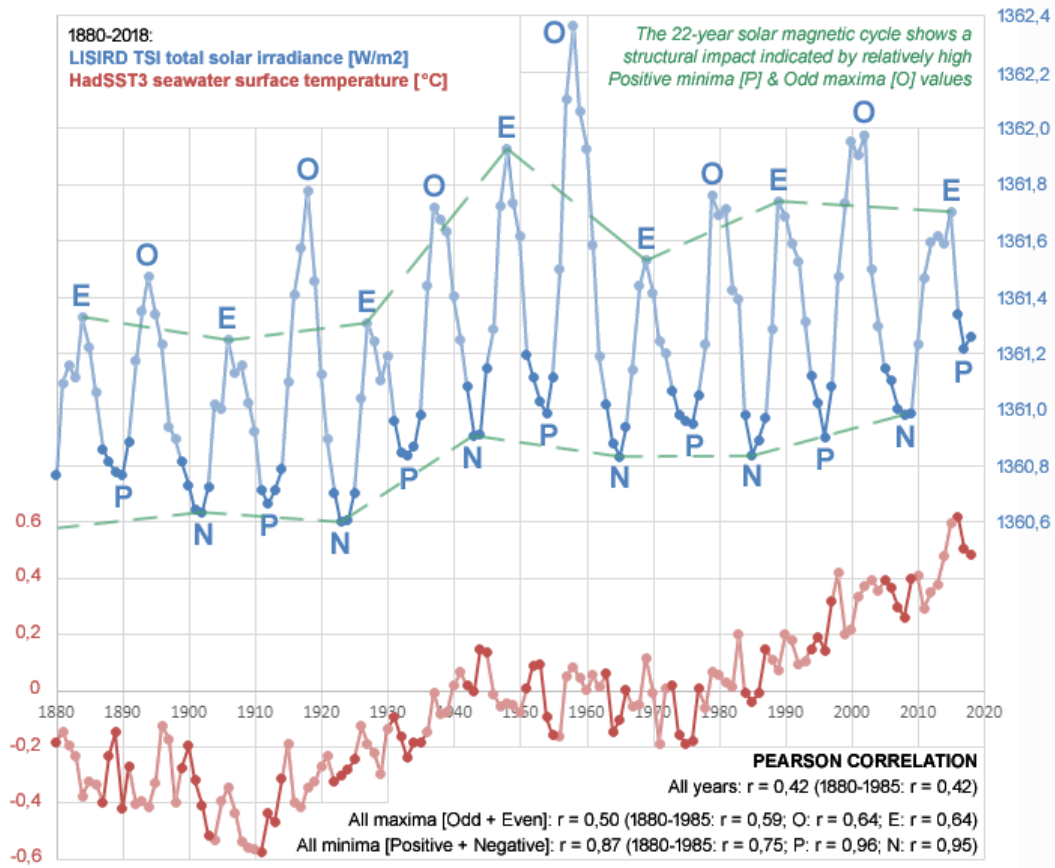


Figure 2. The individual phases of the solar cycle show correlations for the LISIRD TSI total solar irradiance and HadSST3 seawater surface temperature that are significantly higher compared to the values for the entire cycle. The minima show structurally higher correlation values with respect to the maxima. The TSI has a structural impact due to the 22-year magnetic solar cycle, which is expressed in relatively high 'positive TSI minima' [P] and 'odd TSI maxima' [O] (relative to in respective the 'negative TSI minima' [N] and 'even TSI maxima' [E]). This structural phenomenon is in accordance with the Gnevyshev-Ohl rule, which is associated with just the maxima of the sunspot cycle according the literature (Zolotova & Ponyavin, 2015).

3.1 Total solar irradiance (TSI) & temperature correlate higher during minima than during maxima

Figure 2 describes a stable correlation ($r = 0,42$) for the TSI and seawater surface temperature showing the same magnitude for both the period 1890-1985 and the period 1880-2018. However, for both the minima and maxima of the solar cycle the correlations

are at a significantly higher level; in accordance with expectations (Hiyabara et al., 2008), the correlation for the individual phases shows the highest level for the minima.

Moreover, correlations at both the positive & negative minima and the odd & even maxima reach an even higher level. For the period 1880-1985, very high correlations with almost the same value are found for both the positive and negative minima. And for the odd and even maxima the same correlation value is found. This indicates that during the course of the 22-year cycle, the fluctuation of the TSI-temperature correlation shows a high degree of regularity.

The structurally higher correlations in the positive and negative minima series (compared to the combination of both series) appear also directly related to the Gnevyshev-Ohl rule; in figure 2 the dashed green curves show the impact for both the TSI minimums and the TSI maximums separately.

3.2 Temperature profile for the 22-year & 11-year solar cycle

The HadSST3 seawater surface temperature profile for the 22-year solar cycle has been determined based on the period 1882-1988. This period includes: 5 even maximums, 5 positive minimums, 5 odd maximums, and 5 negative minimums. The mean values for these 4 categories serve each as a separate reference point. The average value is then determined for the years around each of these 4 reference points. This results in 4 reference profiles that each show a temperature difference within the range of 0,20-0,27 °C that manifest in 7 to at most 11 years (with an average value of 0,236 °C). The trend has subsequently been removed from each of the 4 reference profiles. Finally, the temperature profile is compiled by means of the years around the 4 reference points. In particular the years around the minimum reference points have been used for this because the years around the two maximum reference points show less consistency compared to the other 2 reference profiles (the method section describes the procedure in detail). The profile for the 11-year Schwabe cycle is derived from the profile of the Hale cycle; only the minima of the Hale temperature profile served as reference points.

The temperature profile for the Hale cycle is shown in figure 3. The length of the Hale profile is only 21 years because the Hale cycles in the research period were relatively short: the average length of the Hale cycles in the period 1890-1985 is approximately 21 years. For the Hale cycle profile, the largest temperature difference is found between the positive minimum and the phase that follows 2 years before the negative minimum. The (average) temperature difference between the positive minimum and the temperature peak is 0,215 °C. The temperature difference between the positive minimum and the negative minimum is 0,059 °C.

The TSI odd maximum occurs 4 years after the TSI positive minimum and the TSI even maximum occurs 5 years after the TSI negative minimum. So, the TSI even maximum coincides with the highest temperature value in the 2nd part of the Hale cycle (which starts from the negative minimum and ends at the positive minimum).

Figure 3 shows that the first part and the second part of the Hale cycle show an asymmetrical temperature trend. During the first part, the fluctuations are more frequent and the amplitude is higher relative to the second part. The temperature peaks relatively late in the first part and it peaks relatively early in the second part. In addition, the profile of the Hale cycle shows an oscillation with fluctuations that take 2 to 7 years, which corresponds to the variation described for the duration of the ENSO cycle. This is not entirely surprising as it is known that there are strong statistical relationships between ENSO and the activity of the Sun (Narsimha & Bhattacharyya, 2010).

For the period 1882-1988, the radiative forcing between all adjacent maxima and minima shows an average value of 0,86 W/m². Combined with the average maximum

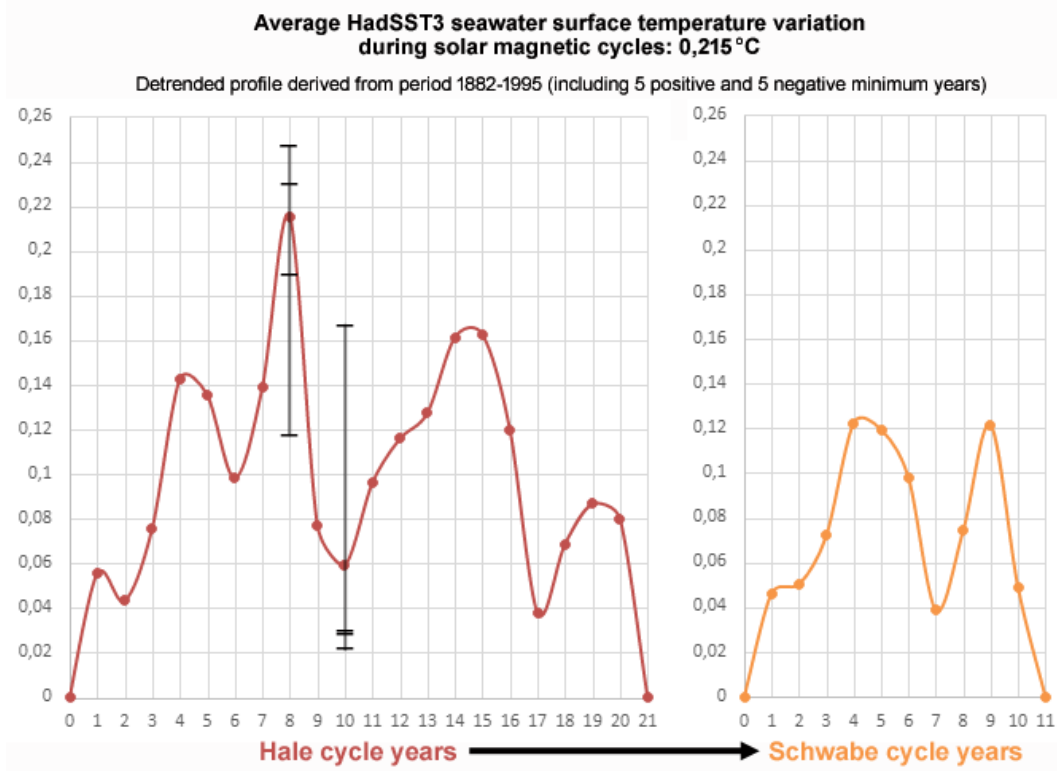


Figure 3. Seawater surface temperature profile for the Hale cycle based on the period 1882-1988 (which includes e.g. 5 positive minima and 5 negative minima) shows a maximum impact of 0,215 °C. During the first part of the Hale cycle, the fluctuations are larger than during the second part. The temperature profile for the Schwabe cycle shows a maximum impact for seawater surface temperature of only 0,122 °C. The bandwidths shown for the negative minimum year and temperature peak year (which is found 2 years before the negative minimum year) represent the outliers are derived from 4 successive full Hale cycles based on the period 1890-1976 (solar cycles 13-20) - which involves less data than the temperature profile itself, nevertheless, the 4 values average result is for both phases of the cycle approximately similar to the profile value.

temperature difference within the profile of 0,215 °C this results in a solar sensitivity within the Hale cycle of 0,25 °C per W/m² at the top of the atmosphere (TOA); converted to Earth's surface this results in a value of 1,43 °C per W/m² (via a conversion factor of 0,175: 25% based on Earth's spherical formation in combination with 70% albedo). However, the impact of an amplifying factor for the TSI signal at the top of the atmosphere has not yet been taken into account in this latter result. In the section discussion & conclusion an amplification factor with a value of 6 is used in order to find the solar sensitivity on Earth's surface for the Hale cycle, which results in a value of 0,238 °C per W/m². Likewise, for the 11-year cycle a considerably lower solar sensitivity on Earth's surface is found: 0,135 °C per W/m². Within the conceptual framework of the IPCC, both the 22-year Hale cycle and the amplification factor are being ignored (IPCC, 2013).

For the sake of completeness, figure 3 also shows the temperature profile for the 11-year Schwabe cycle (which has been derived directly from the Hale cycle profile). A striking feature of the profile for the Schwabe cycle is that it contains 2 peaks of approximately the same height. This finding is not entirely surprising neither because of the fact that for the 11-year sunspot cycle 2 maxima are also described - which typically arise

in a time frame of 2 to 4 years. This period between the two peaks is known as the 'Gnevyshev gap'; the relative height of the peaks relates to Forbus decreases (which involves rapid decreases in cosmic rays intensity following coronal mass injection) and is indicative for an odd/even cycle (Ahluwalia et al., 2008). In the literature the first sunspots peak relates to UV radiation and the second peak to geomagnetic disturbances (+ aurora phenomena) (Gnevyshev, 1977).

3.3 Positive & negative TSI minima show high correlation with seawater surface temperature

The upper part of figure 4 describes for the period 1890-1985 a high correlation for TSI and seawater surface temperature with a declared variance of around 90% for both the positive and negative minima. This involves the same correlations that are described for the minima in figure 2; in figure 4 the TSI scale has been adjusted to show the dynamics visually. For the positive and negative minima separately, the temperature follows the trend of the TSI (with exception for the first transition of the negative minima where both factors move in opposite directions). However, when the distinction between the positive and negative minima is ignored, 6 out of 9 transitions show an opposite movement between the TSI and the temperature. This dynamic for the combination is inconsistent with the dynamics for the positive and negative minima separately.

The introduction section describes that during the minima of the positive phase temperature typically reaches the lowest level since the Maunder minimum. Regarding the physical mechanism involved it is known that during the negative phase of the solar cycle the supply of cosmic rays (which is associated with cloud formation (Svensmark, 2015)) is more sensitive because then the supply comes more via the equator of the Sun, while during the positive phase the supply comes more via the poles (Hiyehara et al., 2008). This implies that based on the direction of cosmic rays supply one can conclude that the relationship between TSI and temperature directly depends on the polarity of the Sun. During the negative phase (which starts at around the odd maximum, during the transition from the positive minimum to the negative minimum) a relatively small amount of energy is needed for a temperature increase, while during the positive phase (which starts around the even maximum, during the transition from the negative minimum to the positive minimum) more energy is required for the same temperature rise. Logically this means that a structural correction is needed to describe (and better understand) the relationship between the TSI and the temperature - although the use of a correction is not necessary for a comparison between individual years when these involve the same phase of the 22 year cycle.

In the bottom part of figure 4 a correction has been applied to the negative TSI minimum values. Due to the correction the correlation for the combination of the positive and negative minimum values shows the mean value of both minima phases separately. This result implicates that in the bottom part of figure 4 the explained variance for the combination ends up at a likewise high percentage (90,5%) as seen for both minima separately, while in the top part of figure 4 the explained variance is much lower (56,6%). In addition, after using the correction the TSI and temperature move in the same direction at all 9 transitions. The solar sensitivity for the combination is 1,20 °C per W/m² at the top of the atmosphere (TOA); converted to Earth's surface this produces a value of 6,86 °C per W/m². However, this does not yet take into account the influence of the amplifying factor on the TSI signal at the top of the atmosphere; the discussion & conclusion section assumes an amplification value of 6 which results in a solar sensitivity on Earth's surface of: 1,143 °C per W/m² ($= 1,20 / ((0,25 \times 0,70) * 6)$), which is only slightly lower than the value at the top of the atmosphere.

The solar sensitivity of 1,20 °C per W/m² TOA (for Earth's surface: 1,143 °C per W/m²) for the period 1890-1985 combined with the solar sensitivity during the 22-year

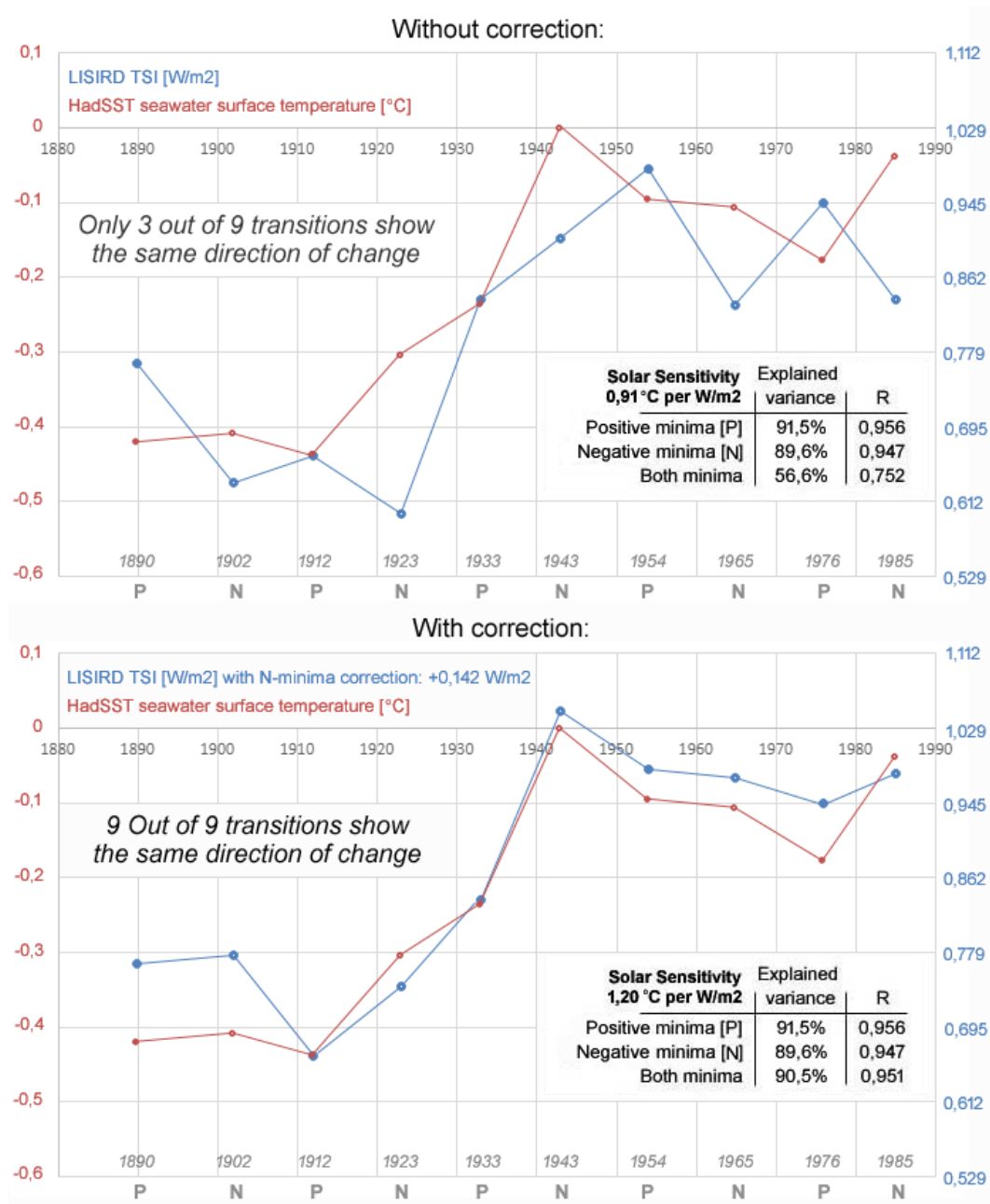


Figure 4. (top) HadSST3 seawater surface temperature plotted against LISIRD TSI (+1360 W/m²) shows that for the period 1890-1985 very high correlations are only found for the positive [P] and negative [N] minima separately; (bottom) after a correction of +0,142 W/m² focused on the negative TSI values, a very high correlation is also found for the combination of the minima. With the use of a regression analysis, the solar sensitivity at the top of the atmosphere (TOA) for this period is established at: 1,20 °C per W/m² for the LISIRD TSI values above 1360 W/m² (based on a declared variance of 90,5%). The values for the minimum year 1912 have been used as reference point.

solar cycle of 0,25 °C per W/m² TOA (for Earth's surface: 0,238 °C per W/m²) implies that the long-term solar sensitivity is 4,8x higher than during the short-term perspec-

tive of the 22-year cycle. Compared to the 11-year cycle the long-term solar sensitivity is 8,4x higher.

According the LISIRD TSI dataset, the total solar irradiance between Maunder minimum (1360,274 W/m² TOA) and the most recent positive minimum year 2017 (1361,215 W/m² TOA) has increased by 0,941 W/m² TOA. Based on the long-term solar sensitivity of 1,143 °C per W/m² after taking into account Earth's shape (25%), albedo (70%) and the amplifying factor (6x) for the TSI signal, this results in a temperature rise at Earth's surface of 1,07 °C (based on the TSI signal of 1,20 °C per W/m² TOA, the value is slightly higher: 1,13 °C).

For the positive and negative minima separately, the solar sensitivity (TOA) is in respective: 1,10 °C per W/m² and 1,22 °C per W/m².

The magnitude of the correction is with a value of more than 0,1 W/m² about one tenth of the average fluctuation of the TSI during an 11/22 year solar cycle. This represents the same magnitude found at the structural variations of the sunspot cycle based on the Gnevyshev-Ohl rule (Zolotova & Ponyavin, 2015).

3.4 Multi-year TSI minima show a comparable trend with seawater surface temperature after correction

The correction method aimed at the negative TSI minimum values has also been applied to the minima based on the 3-year, 5-year, 7-year, 9-year and 11-year average values (which involve both sides surrounding the minimum).

Figure 5 shows that the magnitude of the correction for the 3-year to the 9-year average is slightly smaller (0,110-0,138 W/m²) than the correction value for the 1-year minima (0,142 W/m²), but the values show consistently the same order of magnitude. The 11-year average shows an even smaller correction value (0,100 W/m²); however, because there is an overlap between various periods the result for the 11-year period is disregarded in this analysis.

Figure 5 shows for the 1-year to 9-year minima that the first five values of both the LISIRD TSI and the seawater surface temperature are lower than the last five minima. Also, the first five values always show the lowest value at 1912 and the highest value at 1933; for the last five values the year 1976 always shows the lowest value.

Only the 1-year to 5-year minima show the same direction of the trend at all 9 transitions for the LISIRD TSI and the HadSST3 seawater surface temperature after applying the negative TSI correction. For the 7-year and 9-year minima, eight out of nine transitions show the same trend direction; only the transition between 1943 and 1954 shows opposite trends. Figure 2 presents an explanation for this exception because the 1958 maximum (+ the immediately surrounding years) is the largest outlier in the LISIRD TSI dataset. This phenomenon also explains why in figure 5 the highest average TSI value is found at the 1954 minimum for both the 7-year and 9-year average, while the 1-year to 5-year show the highest level for both the TSI and the temperature at the 1943-value.

For the 1-year to 9-year minima, the explained variance is within the bandwidth of 89.2-92.8% after applying the correction aimed at the negative minima. With increasing length of the minima periods the value of the explained variance fluctuates only a few percent from the 90,5% explained variance found at the 1-year minima for the positive and negative minima separately, as well as for the combination of both minima including the correction. Correlation significance levels show that the results are highly significant [p=0,000] for all minima periods shown in figure 5.

When the correction value based on the 1-year minima period (0,142 W/m²) would have been applied to all other perspectives, only the explained variance for the 3-year

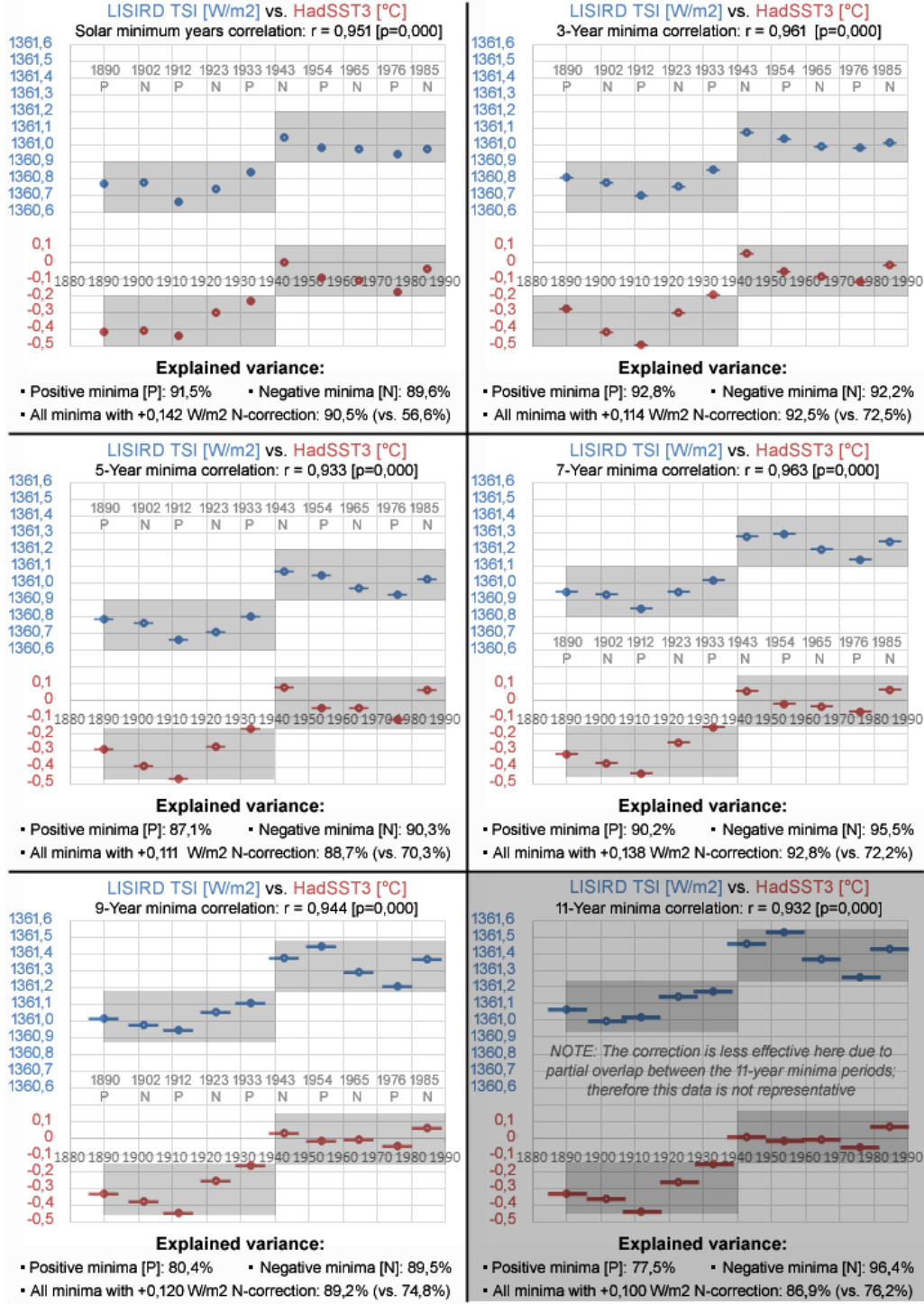


Figure 5. After applying a correction aimed at the negative minima, the 1-year, 3-year, 5-year, 7-year, and 9-year periods around the minima show similar dynamics. The first 5 values of both the LISIRD TSI and the HadSST3 are below the last 5 values. For the first 5 values the 1912 minimum always shows the lowest value and the 1933 minimum shows the highest value; for the last 5 values the 1976 minimum always shows the lowest value.

period would show a small drop (from 92,5% to 92,4%). The 5-year to 9-year periods would then show a further rise for the explained variance.

4 Discussion & Conclusions

This article investigates the Sun's impact on climate with the 22-year magnetic solar cycle. The solar sensitivity is described in 3 forms: (1) in terms of the TSI at the top of the atmosphere; (2) this value is then converted to Earth's surface via a correction for the spherical Earth (25%) and the albedo factor (70%); (3) finally, it has also been corrected with an amplifying factor which increases the temperature impact of the TSI signal at the top of the atmosphere.

For a calculation of the temperature impact of the Sun over a certain period, it is not strictly necessary to make the conversion to Earth's surface when phase differences within the 22-year cycle are taken into account. However, this conversion does become necessary for a description of the solar sensitivity on Earth's surface in terms of the radiative forcing. Therefore, the impact of the amplification factor will now be discussed in more detail here (without going into the possible physical mechanisms involved).

Since the 1990s experts have speculated about the impact of an amplifying factor for the TSI signal formed by the Sun at the top of the atmosphere. Literature has taken into account the possibility that the magnitude of the amplification factor could theoretically vary at the order of 2 to 10 times (Stott et al., 2003). However, there is no consensus about the exact magnitude; therefore, controversy also exists on this matter. Estimates appear to depend, among other things, on the TSI dataset used (Haigh, 2007).

Based on 20th century data, the estimates range from 2-3 times (Haigh, 2007), 3 times (Stott et al., 2003), 4-6 times (Ziskin & Shaviv, 2012) up to as high as 4-8 times (Holmes, 2018). The IPCC confirms that there is great uncertainty about the radiative forcing of the Sun (Haigh, 2007). The most detailed estimates have been described based on the 11-year solar cycle, where the values for the amplification factor are relatively high: 5-7 times (Shaviv, 2008). As far as is known, there are no descriptions which indicate that there are concrete reasons to assume that the magnitude of the amplifying factor for the TSI signal also fluctuates. Therefore, it is assumed here that there is a stable amplification factor with a value of 6 combined with a bandwidth of 5 to 7.

This implies that the Sun's sensitivity at Earth's surface is (only) slightly lower compared to the value measured at the top of the atmosphere. After all factors have been taken into account, the result via the chosen amplifying value (6 times) amounts to 95% of the TOA value. If the amplification value were slightly lower, then the Earth's surface would have almost the same value as the TSI at the top of the atmosphere (with an amplification value of 5,7 times it would produce almost exactly the same value). The bandwidth for the amplifying factor is used here to describe an indication for the uncertainty margin of the solar sensitivity specific to the perspective of Earth's surface after all factors have been taken into account.

For the three perspectives examined, the following values are found in regard to solar sensitivity:

- 11-year cycle:
 - Solar sensitivity based on just TSI at top of atmosphere [TOA]: 0,142 °C per W/m².
 - Solar sensitivity converted to surface without amplifying factor: 0,81 °C per W/m².
 - Solar sensitivity converted to surface with amplifying factor (5-7 times): 0,135 ± 0,03 °C per W/m².
- 22-year cycle:

- Solar sensitivity based on just TSI at top of atmosphere [TOA]: 0,25 °C per W/m².
- Solar sensitivity converted to surface without amplifying factor: 1,43 °C per W/m².
- Solar sensitivity converted to surface with amplifying factor (5-7 times): 0,238 ± 0,05 °C per W/m².

- Period 1890-1985:

- Solar sensitivity based on just TSI at top of atmosphere [TOA]: 1,20 °C per W/m².
- Solar sensitivity converted to surface without amplifying factor: 6,86 °C per W/m².
- Solar sensitivity converted to surface with amplifying factor (5-7 times): 1,143 ± 0,23 °C per W/m².

This overview shows that the solar sensitivity at Earth's surface depends especially on the magnitude of the amplification factor. The value of the solar sensitivity at Earth's surface increases when the amplifying factor decreases. This also applies to the albedo factor because a lower albedo value leads to a higher result in the calculation of the solar sensitivity for Earth's surface.

This implies that solar sensitivity for the long-term perspective is more than 4 times (4,8 times) higher than during the short-term perspective of the 22-year magnetic solar cycle; when compared with the perspective of the 11-year sunspot cycle, the value for the long-term perspective is more than 8 times (8,4 times) higher. These values are approximately 2 times higher than the ratios described in literature relative to the 11-year solar cycle (de Jager et al., 2006; Shaviv, 2005, 2012). These results also confirm earlier descriptions based on periods that go further back in time, which show that the temperature impact during the 22-year cycle is much larger (here 78%) than during the 11-year cycle; in a study by Scafetta & West (Scafetta, 2005) a 54% higher value is reported for the 22-year cycle ($0,17 \pm 0,06$ °C per W/m²) versus the 11-year cycle ($0,11 \pm 0,02$ °C per W/m²). Related literature also confirms that the change of magnetic polarity plays a key role in this (Hiyehara et al., 2008).

The IPCC describes in AR5 (2013) a temperature effect for the 11-year cycle with fluctuations at the order of 0,03-0,07 °C (mean value 0,05 °C) (IPCC, 2013); the temperature profile for the 11-year cycle in figure 3 shows fluctuations with an average value of 0,122 °C which is more than 2 times higher than the IPCC description.

Based on long-term solar sensitivity, it has been calculated that the Sun can be held responsible for a temperature rise of approximately 1,1 °C since Maunder minimum (late 17th century). Estimates for the total warming since Maunder minimum are in the order of 1,5 °C (PAGES2k Consortium, 2019). Estimates for the temperature difference between a passive and active Sun are in the order of 1 °C (Shaviv, 2012) (up to 2 °C). Since the start of the Holocene 11,700 years ago, the activity of the Sun has shown the highest change between Maunder minimum and the early 21st century (Usoskin et al., 2007). An estimate is also available which describes that the increase in solar activity since the emergence of life on Earth can explain about half to 2/3 of the temperature increase (Karoff & Svensmark, 2010; Scafetta, 2013). These estimates are consistent with the long-term solar sensitivity described here based on the period 1890-1985.

Because the solar minimum years do not coincide with the start and end of the 20th century, it is not possible to make an exact calculation based on the minima for the share of the Sun in the seawater surface temperature rise between 1900 and 2000, which is about 0,416 °C. However, an indicative calculation can be made on the basis of the negative minima in the period 1902-2008 (this period covers almost the entire 20th century). For the proportion of the Sun, the percentage here amounts to 62,1% of the 0,671 °C warming of the seawater surface temperature between 1902 and 2008; this percentage is not far below the upper limit of 69% described by Scafetta & West for the period 1900-2005 (Scafetta & West, 2008). For the period 1890-2017 the Sun provides a share of 58,2% in the warming of 0,928 °C. Both percentages are around 60% - just below the upper

limit of 64% of the bandwidth described in the introduction for the global warming in the 20th century (Scafetta, 2013).

For the 21st century, a comparison between the positive minimum years 1996 and 2017 provides a remarkable picture, because based on the solar sensitivity of $1,2 \text{ }^{\circ}\text{C per W/m}^2$ the entire temperature rise (103.6%) is explained by the Sun. However, a comparison between the positive minimum years 1954 and 2017 yields a percentage of the sun that is less than half (46.4%).

From an energetic point of view, the solar sensitivity for the long-term perspective at Earth's surface (with the amplification factor included) shows with a value of $1,143 \pm 0,23 \text{ }^{\circ}\text{C per W/m}^2$ a measure for the equilibrium climate sensitivity parameter (λ). The temperature impact of this is comparable to a climate sensitivity for the doubling of CO₂ with a bandwidth of $3,38\text{-}5,08 \text{ }^{\circ}\text{C}$ (based on: $3,7 \text{ W/m}^2 \times 1,143 \pm 0,23 \text{ }^{\circ}\text{C per W/m}^2$). The midpoint of this bandwidth is found at the value $4,23 \text{ }^{\circ}\text{C}$, which is below the upper limit of the bandwidth that the IPCC applies for climate sensitivity: $1,5\text{-}4,5 \text{ }^{\circ}\text{C}$ (IPCC, 2013). An additional comment follows based on the period 1912-1965.

Based on the dynamics in the lower part of figure 4, the period 1912-1965 shows an almost perfect correlation (combined with an explained variance of 99%) between the minimum values of LISIRD TSI and HadSST3 seawater surface temperature. If the calculation had been made on the basis of the period 1912-1965, the solar sensitivity would drop from $1,20 \text{ }^{\circ}\text{C per W/m}^2$ to $1,05 \text{ }^{\circ}\text{C per W/m}^2$ (with the use of an unchanged correction aimed at the negative minima of $0,142 \text{ W/m}^2$). The warming after the Maunder minimum would then amount to $0,99 \text{ }^{\circ}\text{C}$ based on the period 1912-1965 and the solar sensitivity would amount to $1,00 \pm 0,20 \text{ }^{\circ}\text{C per W/m}^2$ based on the amplifying factor (6x). This is energetically comparable to a climate sensitivity for doubling CO₂ with a bandwidth of $2,96\text{-}4,44 \text{ }^{\circ}\text{C}$. This bandwidth corresponds to the upper side of the IPCC bandwidth. The explained variance of 99% for the 53-year period 1912-1965 offers hardly any impact for influences other than the Sun. This suggests that the Sun is most likely responsible for the temperature trend at least until 1965. Based on the period 1912-1965 the solar sensitivity for the long-term perspective is 4,2 times higher than the short-term perspective of the 22-year cycle and 7,4 times higher than the short-term perspective of the 11-year cycle.

The correction shows that there is an opposite temperature effect present around the phenomenon related to the Gnevyshev-Ohl rule. Moreover, the phenomenon itself applies to both the TSI maximums and the TSI minimums in the full period starting from 1880 (see figure 2). The SATIRE-T TSI dataset (Wu et al., 2018) shows that the relatively low negative TSI minima involve a pattern which origins from the ER magnetic flux (ephemeral regions); the pattern is not present in the AR magnetic flux (active regions - which strongly correlate with sunspots and F10.7 radio flux [http://lasp.colorado.edu/lisird/data/noaa_radio_flux/] (NOAA, 2018))), nor in the open magnetic flux (coronal source flux). ER magnetic flux is missing in early TSI reconstruction methods (Lean et al., 1995; Hoyt & Schatten, 1993), which explains why the pattern is not present in those datasets. The SATIRE dataset also serves for CMIP6 modellers (Matthes et al., 2017). The top of figure 6 displays the sunspot cycle (which shows the 11-year periodicity of the Schwabe cycle); the bottom of figure 6 displays the cosmic ray flux, which shows an 22-year alternating pattern of flat ($q_A > 0$) and peaked ($q_A < 0$) tops that coincides with the solar minima of the sunspots cycle.

The magnitude of the correction appears to be more or less independent of the length of the minimum period used in the calculation; the bandwidth of the correction ranges from $0,110\text{-}0,148 \text{ W/m}^2$ for the values based on 1 to 9 year periods around the TSI minima. This means that there is a structural temperature effect that, in terms of magnitude, approximately corresponds to the average impact of the fluctuations based on the Gnevyshev-Ohl rule. The direction of the temperature effect can be explained on the ba-

sis of a sensitivity difference for the influence of cosmic rays during the positive and negative phase of the Hale cycle (Hiyahara et al., 2008). During the negative phase, the climate is more sensitive to the supply of cosmic rays than during the positive phase. The negative minimum falls in the middle of the negative phase (see figure 1). As a result the influence of the loss of cosmic radiation due to the poloidal maximum is relatively large, which results in relatively high temperatures during the negative TSI minima. Both the mechanism involved with this temperature effect (as a result of the change of the magnetic solar poles), as well as the magnitude of the associated impact of the temperature effect (comparable with the impact of the Gnevyshev-Ohl rule) have been identified by approximate.

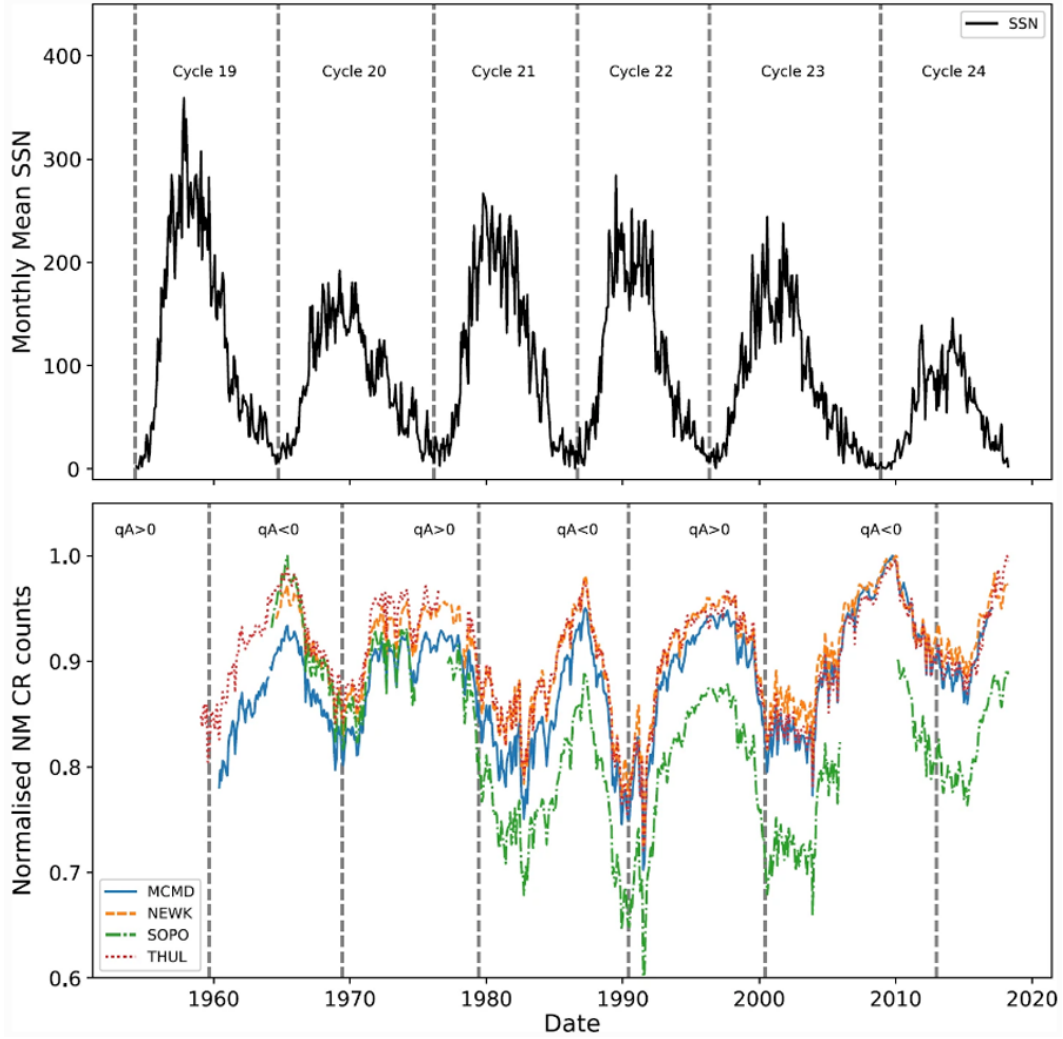


Figure 6. The 11-year periodicity of the Schwabe cycle based on sunspots (top); the 22-periodicity of cosmic rays flux indicated by flat [$qA > 0$] and peaked [$qA < 0$] tops (bottom) (Ross & Chaplin, 2019).

The temperature development might be directly related to background solar irradiance [BSI], which concerns the radiation of the Sun excluding the influence of solar flares and sunspots. BSI involves a dynamic component on top of the base level in the signal from the Sun measured at the top of the atmosphere. Uncertainty margins for the baseline (which itself is estimated at around 1361 W/m² since 2008) are significantly lower

than for the TSI fluctuations which arise from magnetic activity due to solar flares [T_F] and sunspots [T_S]. This might also explain why the correlation between sunspots and temperature is low; for, both do not involve the background component at all. Equation (1) (Lean et al., 1995) defines that TSI [$T(t)$] represents the sum of different components. Equation (1) contains only 2 magnetic components, which is in accordance with the Lean method (Coddington et al., 2016); however, a dynamic BSI component that fluctuates over time on top of the base level component [T_Q] is missing:

$$T(t) = T_Q + \Delta T_F(t) + \Delta T_S(t) \quad (1)$$

For the period 1890-1985, the LISIRD TSI dataset shows high correlations with the NRLTSI2 dataset (0,903), IPCC AR5 dataset (0,938) and Satire S&T dataset (0,944). Correlations among the other 3 TSI datasets fall within the bandwidth 0,927-0,998. For the period 1985-2012, the LISIRD TSI dataset shows a high correlation with the NRLTSI2 dataset (0,961) but lower correlations are found with the IPCC AR5 dataset (0,846) and Satire S&T dataset (0,868). For this period correlations among the other 3 TSI datasets fall within the bandwidth 0,941-0,984. For the entire period 1890-2012, the LISIRD also shows comparable correlations with the other datasets (0,916-0,926); correlations among the other 3 TSI datasets fall within the bandwidth 0,925-0,995. The period until the year 2012 has been considered here because the IPCC AR5 TSI dataset ends in the year 2012.

The LISIRD dataset shows for the satellite era a continuous upward trend for the TSI minima since the mid-eighties. A similar continuous upward trend for the TSI minima in the satellite era is described by the Belgian RMIB TSI dataset (DeWitte & Nevens, 2016). The authors of both datasets are involved with the Community-Consensus TSI composite, which also shows this trend.

Here the conclusion is made that the Sun is responsible for the formation of an climate oscillation with an upward slope. With consideration of the 22-year TSI cycle, the high explained variances with a bandwidth of 89-93% for the various minimum periods around the period 1890-1985 (99% for the 1912-1965 minima) leave little room for a large influence of other factors, such as CO₂. However, when the 22-year cycle is ignored, it is not possible to notice (nor to describe) this strong relationship between solar activity and temperature.

The IPCC climate models do not take into account temperature effects that arise as a result of: (1) the changes of the magnetic solar poles within the 22-year cycle; the same applies to (2) the influence of an amplifying factor on the impact of the TSI signal at the top of the atmosphere. Climate models also do not take into account the dynamics that ensure that (3) the solar sensitivity within the 11-year TSI cycle is significantly lower than in the multi-decadal long-term perspective. In determining short-term trends, climate models neither take into account (4) the impact of the upward phase of the multi-decadal cycle, which can be directly connected with the Gleissberg cycle minima of the Sun (Feynman & Ruzmaikin, 2014), nor do climate models consider the influence of very long-term solar related cycles such as for example: Jose cycle 179 years (Jose, 1965), de Vries/Suess cycle 248 years (Holmes, 2018), Eddy cycle 1000 years (Holmes, 2018), and Hallstatt cycle 2400 years (Usoskin et al., 2016) / Bray cycle 2500 years (Holmes, 2018). The missing of this set of 4 solar-related factors in climate models points towards a significant structural underestimation of the Sun's impact on the climate, leading to an overestimation of the impact of CO₂ and other natural greenhouse gases. ENSO and NAO represent two other factors (next to e.g. greenhouse gasses) which are known influence sea surface temperature; however, both factors also show high correlations with solar activity (Kirov & Georgieva, 2002). Fundamentally it is important that the greatest temperature effects due to the change of the magnetic poles can be expected around the solar minima, because during these periods the magnitude of the poloidal magnetic field reaches the highest magnitude - see figure 1. Finally, one side note is made here: for, the influence of mankind on the climate system has become evident particularly through

ozone layer depletion resulting from the use of artificial greenhouse gases (especially CFCs); despite the relatively large influence of the Sun, the impact of anthropogenic influences must therefore be acknowledged.

The following abbreviations are used in this manuscript:

ACRIM	Active Cavity Radiometer Irradiance Monitor Satellite
HadSST	Hadley Centre Sea Surface Temperature
IPCC AR5	Intern. Panel on Climate Change Ass. Report 5 (2013)
KNMI	Koninklijk Nederlands Meteorologisch Instituut
LISIRD	Las Interactive Solar Irradiance Data Center
NIOZ	Nederlands Instituut voor Onderzoek der Zee
NRLTSI	Naval Research Laboratory Total Solar Irradiance
PMOD	Physikalisch Meteorologisches Observatorium Davos
SATIRE	Spectral And Total Irradiance REconstructions
TSI	Total Solar Irradiance
WSO	Wilcox Solar Observatory

Acknowledgments

The author gratefully acknowledges the efforts of various informal reviewers from The Netherlands who provided much useful advice.

Funding:

This research received no funding.

Disclosure of Potential Conflicts of Interest:

The author declares no conflict of interest.

Electronic Supplementary Material:

The data analysis is available as a spreadsheet in:

- Excel format (Manuscript-datasheet-Excel.xlsx file: data with calculations).
- CSV format (Manuscript-datasheet-CSV.csv file: data without calculations).

Files are available at url: <https://osf.io/qk9sm/files/>

References

- Ahluwalia, H. S., Kritchfield, K., Ygbuhay, R., & Kamide, Y. (2008). Gnevyshev gap in the annual frequency distribution of cosmic ray decreases and Ap index. In R. Caballero, J. C. D'Olivo, G. Medina-Tanco, L. Nellen, F. A. Sanchez, & J. F. Valdes-Galicia (Eds.), *Proceedings of the 30th international cosmic ray conference* (p. 385-388). Mexico City: World Scientific Publishing Co. Pte. Ltd. Retrieved from https://www.researchgate.net/profile/Roger_Ygbuhay/publication/252722756_Gnevyshev_gap_in_the_annual_frequency_distribution_of_cosmic_ray_decreases_and_Ap_index/links/53d325950cf220632f3cc7f1/Gnevyshev-gap-in-the-annual-frequency-distribution-of-cosmic-ray-decreases-and-Ap-index.pdf
- Camp, C. D., & Tung, K. K. (2007). Surface warming by the solar cycle as revealed by the composite mean difference projection. *Geophys. Res. Lett.*, *34*, L14703. doi: <https://doi.org/10.1029/2007gl030207>

- Cheng, L., Zhu, J., Abraham, J., Trenberth, K. E., Fasullo, J. T., Zhang, B., ...
Song, X. (2019). 2018 Continues Record Global Ocean Warming. *Adv. Atmos. Sci.*, *36*, 249-252. doi: <https://doi.org/10.1007/s00376-019-8276-x>
- Coddington, O., Lean, J. L., Pilewskie, P., Snow, M., & Lindholm, D. (2016). A solar irradiance climate data record. *Bull. Amer. Meteor. Soc.*, *97*, 1265-1282. doi: <https://dx.doi.org/10.1175/bams-d-14-00265.1>
- de Jager, C., Versteegh, G. M., & van Dorland, R. (2006). *Climate Change Scientific Assessment and Policy Analysis - Scientific Assessment of Solar Induced Climate Change* (R. van Dorland, Ed.). de Bilt: Netherlands Environmental Assessment Agency. Retrieved from https://www.pbl.nl/sites/default/files/downloads/500102001_0.pdf
- DeWitte, S., & Nevens, S. (2016). The total solar irradiance climate data record. *The Astrophysical Journal*, *830*, 25. doi: <http://dx.doi.org/10.3847/0004-637X/830/1/25>
- Dudok de Wit, T., Kopp, G., Frölich, C., & Schöll, M. (2017). Methodology to create a new total solar irradiance record: Making a composite out of multiple data records. *Geophys. Res. Lett.*, *44*, 1196-1203. doi: <https://doi.org/10.1002/2016GL071866>
- Feynman, J., & Ruzmaikin, A. (2014). The Centennial Gleissberg Cycle and its association with extended minima. *J. Geophys. Res.-SPACE*, *119*, 6027-6041. doi: <https://dx.doi.org/10.1002/2013jA019478>
- Gnevyshev, M. N. (1977). Essential features of the 11-year solar cycle. *Sol. Phys.*, *51*, 175-183. Retrieved from <http://adsabs.harvard.edu/full/1977SoPh...51..175G>
- Haigh, J. D. (2007). The Sun and the Earth's Climate. *Living Rev. Sol. Phys.*, *4*, 1-64. doi: <https://dx.doi.org/10.12942/lrsp-2007-2>
- Hale, G. E. (1908). On the probable existence of a magnetic field in sun-spots. *Astrophys. J.*, *28*, 315-343. Retrieved from <http://articles.adsabs.harvard.edu/full/1908ApJ...28..315H/0000315.000.html>
- Hiyahara, H., Yokoyama, Y., & Masuda, K. (2008). Possible link between multi-decadal climate cycles and periodic reversals of solar magnetic field polarity. *Earth Planet. Sci. Lett.*, *272*, 290-295. doi: <https://doi.org/10.1016/j.epsl.2008.04.050>
- Holmes, R. I. (2018). Thermal Enhancement on Planetary Bodies and the Relevance of the Molar Mass Version of the Ideal Gas Law to the Null Hypothesis of Climate Change. *Earth Sci.*, *7*, 107-123. doi: <https://doi.org/10.11648/j.earth.20180703.13>
- Hoyt, D. V., & Schatten, K. H. (1993). A Discussion of Plausible Solar Irradiance Variations, 1700-1992. *J. Geophys. Res.-SPACE*, *98*, 18,895-18,906. doi: <https://doi.org/10.1029/93ja01944>
- IPCC. (2013). *Climate Change 2013: The Physical Science Basis. Contribution of Working Group I to the Fifth Assessment Report of the Intergovernmental Panel on Climate Change* (T. F. Stocker et al., Eds.). Cambridge, United Kingdom and New York, NY, USA: Cambridge University Press. Retrieved from https://www.ipcc.ch/site/assets/uploads/2018/02/WG1AR5_all_final.pdf (Citations: page 56 (Technical Summary): "Longer term forcing is typically estimated by comparison of solar minima (during which variability is least)." Citation page 689 (Chapter 8): "The year 1750, which is used as the preindustrial reference for estimating RF, corresponds to a maximum of the 11-year SC. Trend analysis are usually performed over the minima of the solar cycles that are more stable. For such trend estimates, it is then better to use the closest SC minimum, which is in 1745. ... Maxima to maxima RF give a higher estimate than minima to minima RF, but the latter is more relevant for changes in solar activity.")
- Jose, P. D. (1965). Sun's motion and sunspots. *Astron. J.*, *70*, 193-200. doi:

- https://dx.doi.org/10.1086/109714
- Karoff, C., & Svensmark, H. (2010). How did the Sun affect the climate when life evolved on the Earth? - A case study on the young solar twin $\kappa 1$ Ceti. *arXiv preprint*, 1-5. Retrieved from <https://arxiv.org/pdf/1003.6043.pdf>
- Kirov, B., & Georgieva, K. (2002). Long-term variations and interrelations of ENSO, NAO and solar activity. *Phys. Gem. Earth*, 27, 441-448. doi: [https://doi.org/10.1016/S1474-7065\(02\)00024-4](https://doi.org/10.1016/S1474-7065(02)00024-4)
- Kopp, G. (2019). *Historical total solar irradiance reconstruction, time series*. Retrieved from http://lasp.colorado.edu/lisird/data/historical_tsi/
- Kopp, G., Krivova, N., Wu, C. J., & Lean, J. (2016). The Impact of the Revised Sunspot Record on Solar Irradiance Reconstructions. *Sol. Phys.*, 291, 2951-2965. doi: <https://doi.org/10.1007/s11207-016-0853-x>
- Lean, J., Beer, J., & Bradley, R. (1995). Reconstruction of solar irradiance since 1610: Implications for climate change. *Geophys. Res. Lett.*, 22, 3195-3198. doi: <https://doi.org/10.1029/95gl03093>
- Matthes, K., Funke, B., Andersson, M., Barnard, L., Beer, J., & Charbonneau, P. (2017). Solar forcing for CMIP6 (v3.2). *Geosci. Model Dev.*, 10, 2247-2302. doi: <https://doi.org/10.5194/gmd-10-2247-2017>
- MetOffice. (2020). *Met office hadley centre observations datasets: time series (annual globe)*. Retrieved from <https://www.metoffice.gov.uk/hadobs/hadsst3/data/download.html>
- Mursula, K., & Hiltula, T. (2003). Bashful ballerina: Southward shifted heliospheric current sheet. *Geophys. Res. Lett.*, 30, 2135. doi: <https://doi.org/10.1029/2003GL018201>
- Narsimha, R., & Bhattacharyya, S. (2010). A wavelet cross-spectral analysis of solar-ENSO-rainfall connections in the Indian monsoons. *Appl. Comput. Harmon. Anal.*, 28, 285-295. doi: <https://doi.org/10.1016/j.acha.2010.02.005>
- NOAA. (2018). *Noaa adjusted solar radio flux at 10.7cm, time series*. Retrieved from http://lasp.colorado.edu/lisird/data/noaa_radio_flux/
- PAGES2k Consortium. (2019). Consistent multi-decadal variability in global temperature reconstructions and simulations over the Common Era (Supplementary Materials). *Nat Geosci.*, 12, 643-649. doi: <https://doi.org/10.1038/s41561-019-0400-0>
- Ross, E., & Chaplin, W. (2019). The Behaviour of Galactic Cosmic-Ray Intensity During Solar Activity Cycle 24. *Sol. Phys.*, 294, 8. doi: <https://doi.org/10.1007/s11207-019-1397-7>
- Scafetta, N. (2005). Estimated solar contribution to the global surface warming using the ACRIM TSI satellite composite. *Geophys. Res. Lett.*, 32, L18713. doi: <https://dx.doi.org/10.1029/2005gl023849>
- Scafetta, N. (2013). Discussion on common errors in analyzing sea level accelerations, solar trends and global warming. *Pattern. Recogn. Phys.*, 1, 37-57. doi: <https://doi.org/10.5194/prp-1-37-2013>
- Scafetta, N., & West, B. J. (2008). Is climate sensitive to solar variability? *Phys. Today*, 61, 50-51. doi: <https://dx.doi.org/10.1063/1.2897951>
- Scafetta, N., Willson, R. C., Lee, J. N., & Wu, D. L. (2019). Modeling Quiet Solar Luminosity Variability from TSI Satellite Measurements and Proxy Models during 1980-2018. *Remote Sens.*, 11, 2569. doi: <https://doi.org/10.3390/rs11212569>
- Shaviv, N. J. (2005). On climate response to changes in the cosmic ray flux and radiative budget. *J. Geophys. Res.-SPACE*, 110, A08105. doi: <https://doi.org/10.1029/2004ja010866>
- Shaviv, N. J. (2008). Using the oceans as a calorimeter to quantify the solar radiative forcing. *J. Geophys. Res.-SPACE*, 113, A11101. doi: <https://doi.org/10.1029/2007JA012989>
- Shaviv, N. J. (2012). The Role of the Solar Forcing in the 20th century climate

- change. In A. Zichichi & R. Ragaini (Eds.), *International seminar on nuclear war and planetary emergencies - 44th session* (p. 279-286). Singapore: World Scientific Publishing Co. Pte. Ltd. Retrieved from <http://citeseerx.ist.psu.edu/viewdoc/download?doi=10.1.1.708.9707&rep=rep1&type=pdf>
- Smith, T. M., & Reynolds, R. W. (2003). Extended Reconstruction of Global Sea Surface Temperatures Based on COADS Data (1854-1997). *J. Clim.*, *16*, 1495-1510. doi: <https://doi.org/10.1175/1520-0442-16.10.1495>
- Solanki, S. K., Krivova, N. A., & Haigh, J. D. (2013). Solar Irradiance Variability and Climate. *Annu. Rev. Astron. Phys.*, *51*, 311-351. doi: <https://doi.org/10.1146/annurev-astro-082812-141007>
- Stott, P. A., Jones, G. S., & Mitchell, J. B. (2003). Do Models Underestimate the Solar Contribution to Recent Climate Change? *J. Clim.*, *16*, 4079-4093. doi: [https://doi.org/10.1175/1520-0442\(2003\)016<4079:dmutsc>2.0.co;2](https://doi.org/10.1175/1520-0442(2003)016<4079:dmutsc>2.0.co;2)
- Svensmark, H. (2015). Cosmic rays, clouds and climate. *Europhys. News*, *46*, 26-29. doi: <https://doi.org/10.1051/epn/2015204>
- Usoskin, I. G., Gallet, Y., Lopes, F., Kovaltsov, G. A., & Hulot, G. (2016). Solar activity during the Holocene: the Hallstatt cycle and its consequence for grand minima and maxima. *Astron. Astrophys.*, *587*, A150. doi: <https://doi.org/10.1051/0004-6361/201527295>
- Usoskin, I. G., Solanki, S. K., & Kovaltsov, G. A. (2007). Grand minima and maxima of solar activity: new observational constraints. *Astron. Astrophys.*, *471*, 301-309. doi: <https://dx.doi.org/10.1051/0004-6361:20077704>
- Wu, C. J., Krivova, N., Solanki, S., & Usoskin, I. (2018). Solar total and spectral irradiance reconstruction over the last 9000 years. *Astron. Astrophys.*, *620*, A120. doi: <https://doi.org/10.1051/0004-6361/201832956>
- Ziskin, S., & Shaviv, N. J. (2012). Quantifying the role of solar radiative forcing over the 20th century. *Adv. Space Res.*, *50*, 762-776. doi: <https://dx.doi.org/10.1016/j.asr.2011.10.009>
- Zolotova, N. V., & Ponyavin, D. I. (2015). The Gnevyshev-Ohl Rule and Its Violations. *Geomagn. Aeron.*, *55*, 902-906. doi: <https://doi.org/10.1134/S0016793215070300>